Heliyon 10 (2024) e40921

Contents lists available at ScienceDirect

Heliyon

journal homepage: www.cell.com/heliyon

Research article

The metabolomics provides insights into the Pacific abalone (*Haliotis discus hannai*) response to low temperature stress

Ang Li [a,b], Jiaqi Li [a,b,**], Yingpu Wang [a,b], Zirong Liu [a,b], Lulei Liu [a,b], Longzhen Liu [a,b], Suyan Xue [a,b], Ling Zhu [a,b], Yuze Mao [a,b,*]

[a] *State Key Laboratory of Mariculture Biobreeding and Sustainable Goods, Yellow Sea Fisheries Research Institute, Chinese Academy of Fishery Sciences, Qingdao, 266071, China*

[b] *Laboratory for Marine Ecology and Environmental Science, Qingdao Marine Science and Technology Center, Qingdao, 266237, China*

ARTICLE INFO

Keywords:
Metabolomics
Low temperature stress
Haliotis discus hannai
Climate change

ABSTRACT

The low temperatures in winter, particularly the cold spells in recent years, have posed significant threats to China's abalone aquaculture industry. The low temperature tolerance of cultured abalone has drawn plenty of attention, but the metabolic response of abalone to low-temperature stress remains unclear. In this study, we investigated the metabolomic analysis of Pacific abalone (*Haliotis discus hannai*) during low-temperature stress. Pacific abalone used two strains of cultured abalone, namely the bottom-sowing cultured strain (DB) and the longline cultured strain (FS), which had different histories of low-temperature acclimation. The results revealed that eight of the top 10 shared differential expression metabolites of the two strains were carbohydrates. According to the results of the Kyoto Encyclopedia of Genes and Genomes (KEGG) metabolic pathway analysis, low-temperature stress primarily affected several metabolic pathways. These pathways include ABC transporters, carbohydrate digestion and absorption, starch and sucrose metabolism, lysine degradation, TCA cycle, the phosphotransferase system, the glucagon signaling pathway and pyruvate metabolism. The results suggest that Pacific abalone primarily regulates the expression of carbohydrates to enhance energy supply and anti-freezing protection. These findings are crucial for understanding the mechanism of low-temperature tolerance in Pacific abalone, and can help optimize culture strategies for high-quality abalone aquaculture development.

1. Introduction

Climate change is one of the major global ecological challenges [1], leading to an increase in the frequency and magnitude of extreme weather events [2,3], including marine heatwaves (MHWs) and marine cold spells (MCSs), which pose a serious threat to marine organisms [4]. The impacts of MHWs have received increasing attention in the context of global warming [5,6], in contrast to the MCSs, which have received less attention [7]. However, the MCSs can also have an impact on mariculture and may result in

* Corresponding author. State Key Laboratory of Mariculture Biobreeding and Sustainable Goods, Yellow Sea Fisheries Research Institute, Chinese Academy of Fishery Sciences, Qingdao, 266071, China.

** Corresponding author. State Key Laboratory of Mariculture Biobreeding and Sustainable Goods, Yellow Sea Fisheries Research Institute, Chinese Academy of Fishery Sciences, Qingdao, 266071, China.

E-mail addresses: lijq@ysfri.ac.cn (J. Li), maoyz@ysfri.ac.cn (Y. Mao).

https://doi.org/10.1016/j.heliyon.2024.e40921
Received 2 September 2024; Received in revised form 8 November 2024; Accepted 3 December 2024

widespread winter mortality of marine organisms [8,9]. Thus, more focus should be placed on cold stress assessments of aquaculture species.

Abalone is one of the most valuable shellfish in the coastal regions of East Asia [10]. Delicious and nutrient-dense, abalone offers premium animal proteins [11] and a range of bioactive compounds with antithrombotic and antioxidant characteristics [12]. In recent years, farmed abalone production has continued to grow to meet the global demand for high-quality seafood [13]. Temperature fluctuations are a key abiotic factor affecting the growth and survival of the Pacific abalone, especially during climate change [14], and outbreaks of the MCSs can have severe adverse effects on marine organisms living in the intertidal zone [15]. The two primary methods of cultivating abalone at the moment are bottom-sowing culture and north-south relay longline culture (transferring abalone to the south for overwintering in winter), which has gradually become the mainstream culture mode since the abnormally low temperatures in the winter of 2010 led to the large-scale mortality of cultured abalone in the main abalone culture areas in China, such as Sanggou Bay. In the north-south relay longline culture, the abalone are grown in suitable water temperature throughout the culture period and have never experienced water temperatures lower than 11 °C. Feedback from abalone farmers indicates that although the abalone have reasonably excellent growth and survival rates, they do not perform as well in bottom-sowing in northern seas. Mass mortality of abalone in winter has become a challenge, causing significant economic losses to the abalone aquaculture industry. However, little is known about the stress response to low temperature stress in Pacific abalone, and understanding the mechanisms by which they respond to cold stress is essential in developing suitable mitigation strategies. Metabolomics can provide the detailed information needed to help reveal the metabolic responses of the Pacific abalone to low-temperature stress and its adaptive mechanisms.

Metabolomics is the scientific study of chemical processes involving metabolites-the small molecule substrates, intermediates, and products of cell metabolism [16]. It is characterized by high sensitivity and high throughput [17]. In recent years, metabolomics technology has been widely used in the field of aquaculture. However, most of the research on temperature stress has focused on the study of the response to high temperature stress, such as oxidative damage, disruption of amino acid and fatty acid metabolism, and a shift from aerobic to anaerobic metabolism in organisms like the abalone (*Haliotis iris*) [18]. High-temperature stress also leads to mitochondrial failure in Pacific abalone, resulting in incomplete mitochondrial oxidative metabolism of amino acids and fatty acids, and a large accumulation of unstable metabolic intermediates in the cells [14]. The response of these life-sustaining metabolites when abalone faces cold stress is still unclear.

Bottom-sowing and longline culture are the primary production methods of Pacific abalone culture. However, there was a significant difference in the total glycogen content of abalone from the two different culture methods. Specifically, in a recent study, we found that the total glycogen content of abalone from bottom-sowing culture was twice as high as that of abalone from longline culture [19]. As bottom-sowing cultured abalone have to deal with low temperature stress during the winter, the elevated glycogen content reminds us that the regulation of carbohydrate expression may be linked to low temperature tolerance. In this study, we used ultrahigh-performance liquid chromatography coupled with quadrupole time-of-flight mass spectrometry (UHPLC-Q-TOF-MS) technique to monitor the changes of relevant metabolites and metabolic pathways in Pacific abalone under low-temperature stress conditions in both bottom-sowing cultured and longline cultured. This may provide new insights into the effects of low-temperature stress in Pacific abalone and provide a theoretical basis for exploring the low-temperature tolerance traits of Pacific abalone as well as its genetic modification.

2. Materials and methods

2.1. Experimental design

The Pacific abalone used in this investigation were provided by Xunshan Group, an abalone farming company located along the coastal area of Sanggou Bay, Shandong, China. The abalone were randomly divided into two groups: the DB strain, which endured low temperatures during winter in Sanggou Bay, and the FS strain experienced comfortable water temperatures during its winter time in Meizhou Bay, Fujian Province. The temperature environments experienced by the two strains of abalone during overwintering differed significantly, with individuals in the DB strain experiencing water temperatures ranging from 0.53 °C to 9.34 °C during overwintering (Fig. S1), whereas the lowest temperatures in the waters where individuals in the FS strain were located were over 11 °C. Twenty abalone from each group were randomly selected. The wet weight of the bottom-sowing abalone was (48.36 ± 9.23) g, and their shell length was (74.09 ± 5.36) mm. The longline cultured abalone had a wet weight of (39.19 ± 4.35) g and a shell length of (71.48 ± 3.07) mm. Both groups of abalone were temporarily cultivated in aquariums for one week, and the water temperature in the tanks was maintained at 20 °C. The water in the tanks was changed once a day during the temporary rearing period. Fresh kelp was fed to the abalone twice a day, and feeding was stopped one day before the initiation of the incubation process.

The experiment consisted of a total of two temperature treatments: one at 20 °C (control) and the other incubated cyclically. The cyclic treatment involved a 3-h low-temperature air exposure at 0 °C, followed by a 9-h low-temperature seawater incubation at 6 °C. This was done for a duration of 96 h to simulate the bottom culture environment during the winter in northern seas. Six abalone were randomly selected from each strain and incubated in the control group for 96 h, while another six individuals from each strain were incubated in the cyclically low temperature treatment for 96 h. At the end of the incubation, the abalone were cut from the abdominal foot muscle with a cross-type cut using a sterilized razor blade, and approximately 5 ml of hemolymph was collected into a centrifuge tube using a rubber-tipped burette, quick-frozen with liquid nitrogen, and then frozen and preserved in an ultra-low-temperature refrigerator at −80 °C (Haier DW-86L626, Qingdao, China). The abalone in the DB strain for the control experiment were recognized as the KBDB group, and the abalone in the cyclically incubated experiment were recognized as the SYDB group. The abalone in the FS strain for the control were recognized as the KBFS group, and the abalone in the cyclically incubated experiment were

recognized as the SYFS group. No abalone died during the incubation process, and all of the hemolymph samples were stored at −80 °C prior to metabolomics analysis.

2.2. Instruments and reagents

We bought an AB Triple TOF 6600 mass spectrometer from AB SCIEX in Boston, USA. We bought the Agilent 1290 Infinity LC from Agilent, located in Santa Clara, USA. We bought the Eppendorf 5430R from Eppendorf in Hamburg, Germany. Amide was acquired from Waters (Milford, USA) by ACQUITY UPLC BEH. The suppliers of ammonium acetate (NH_4AC), acetonitrile, ammonium hydroxide (NH_4OH), and methanol were Sigma Aldrich (Shanghai, China), Merck (Shanghai, China), and Fisher (Shanghai, China).

2.3. Sample collection and preparation

The chelating agent ethylene diamine tetraacetic acid (EDTA) was added to 5 mL Vacutainer tubes containing fasting hemolymph samples, which were centrifuged for 15 min (1500 g, 4 °C). Prior to LC-MS analysis, each 150 μL aliquot of the plasma sample was kept at −80 °C. After thawing the plasma samples at 4 °C, 400 μL of cold methanol/acetonitrile (1: 1, v/v) was combined with 100 μL aliquots to extract the protein. For 20 min, the mixture was centrifuged at 4 °C and 14,000 g. A vacuum centrifuge was used to dry the supernatant. The samples were redissolved in 100 μL of acetonitrile/water (1:1, v/v) solvent for LC-MS analysis. They were then centrifuged at 14000 g for 15 min at 4 °C, and the supernatant was injected.

Quality control (QC) samples were created by pooling 10 μL of each sample and analyzing them with the other samples in order to track the stability and reproducibility of instrument results [20]. Every five samples, the QC samples were routinely inserted and examined.

2.4. LC-MS analysis

Shanghai Applied Protein Technology Co., Ltd. used a quadrupole time-of-flight (AB Triple TOF 6600) in conjunction with UHPLC (1290 Infinity LC, Agilent Technologies) to conduct the analysis. A 2.1 mm × 100 mm ACQUIY UPLC BEH Amide 1.7 μm column was used to examine the samples for HILIC separation [21]. The mobile phase included A = 25 mM ammonium acetate and 25 mM ammonium hydroxide in water, as well as B = acetonitrile, in both the ESI positive and negative modes. With a 3-min re-equilibration time, the gradient was linearly lowered from 95 % B for 0.5 min to 65 % in 6.5 min, 40 % in 1 min and maintained for 1 min, and 95 % in 0.1 min.

The following were the ESI source conditions: IonSpray Voltage Floating (ISVF) ± 5500 V, curtain gas (CUR) of 30, Ion Source Gas1 (Gas1) of 60, and Ion Source Gas2 (Gas2) of 60. The source temperature is 600 °C. The accumulation time for the TOF MS scan was set at 0.20 s/spectra, and the instrument was configured to acquire throughout the m/z range of 60–1000 Da in the MS-only acquisition. The accumulation period for the product ion scan was set at 0.05 s/spectra, and the instrument was configured to acquire across the m/z range of 25–1000 Da in auto MS/MS acquisition. Information dependent acquisition (IDA) is used to obtain the product ion scan, and the high sensitivity option is chosen. The following parameters were established: Decluttering potential (DP), 60 V (+) and −60 V (−); exclude isotopes within 4 Da; candidate ions to monitor every cycle: 10; collision energy (CE) was set at 35 V with ±15 eV.

2.5. Data processing

Prior to being imported into the publicly accessible XCMS program, the raw MS data were transformed into MzXML files using ProteoWizard MSConvert (https://proteowizard.sourceforge.io/download.html) [22]. The settings used for peak selecting were prefilter = c (10, 100), peakwidth = c (10, 60), and centWave m/z = 10 ppm bw = 5, mzwid = 0.025, and minfrac = 0.5 were used for peak grouping. Isotopes and adducts were annotated using CAMERA (Collection of Algorithms of Metabolite profile Annotation). Only variables with more than 50 % of the nonzero measurement values in at least one group were retained in the retrieved ion features. By comparing the accuracy m/z value (<10 ppm) and MS/MS spectra with an internal database created using accessible authentic standards, the compounds' metabolites were identified.

2.6. Statistical analysis

Following sum-normalization, the R package (ropls) [23] was used to examine the processed data. Multivariate data analysis, such as Pareto-scaled principal component analysis (PCA) and orthogonal partial least-squares discriminant analysis (OPLS-DA), were performed on the data. The robustness of the model was assessed using response permutation testing and 7-fold cross-validation. To show each variable's contribution to the classification, the variable significance in the projection (VIP) value was computed for each variable in the OPLS-DA model. The significance of the differences between two sets of independent samples was assessed using the Student's t-test. Significantly altered metabolites were screened using VIP >1 and p-value <0.05 [24].

2.7. Compound identification and pathway analysis

This project adopts the in-house database (Shanghai Applied Protein Technology) [25,26]. Structural identification of metabolites in biological samples is performed by matching the information of the in-house database, including molecular mass (within <10 ppm

error of molecular mass), secondary fragmentation spectra, collision energy, etc. of metabolites in the local database. The identification results are subject to rigorous manual secondary checking and confirmation. The reliability level of metabolite identification is Level 0–2 [27].

Differential metabolites screened by positive and negative modes were combined before pathway enrichment annotation and analysis (https://www. kegg.jp). In this study, the KEGG database was used for comparison and annotation of differential metabolites, and MetaboAnalyst (version 5.0; http://www.metaboanalyst.ca) was used for pathway analysis [28].

3. Results

3.1. Principal component analysis of data

The peaks obtained from the extraction of all test samples and QC samples were analyzed by PCA, and the results of the experiment demonstrated that the QC samples were closely clustered in the cation and anion modes, which indicated that the experiments were reproducible (Fig. 1). The OPLS-DA model was used to screen out differential metabolites. The evaluation parameters of the OPLS-DA model obtained by 7-fold cross-validation are shown in Table 1, and the validity of the model is examined by 200-permutation-test. With the gradual decrease of the permutation retention, the R^2 and Q^2 of the stochastic model gradually decrease, which indicates that the model is robust and does not suffer from the phenomenon of overfitting. Overall, the data of this experiment were stable and reliable, and the differences in metabolic profiles obtained in the experiment could reflect the biological differences between the samples themselves.

3.2. Differential metabolite screening

A total of 1592 metabolites were identified in this experiment, which were screened for differential metabolites by combining the OPLS-DA model and analysis of variance (one-way ANOVA), with the screening criteria of OPLS-DA VIP >1 and p-value <0.05. A total of 87 (63 in POS and 24 in NEG) differential metabolites were detected by KBDB vs KBFS, which contained 60 (38 in POS and 22 in NEG) up-regulated differential metabolites and 27 (25 in POS and 2 in NEG) down-regulated differential metabolites (Fig. 2A and B). A total of 109 (77 in POS and 32 in NEG) different metabolites were detected in SYDB vs KBDB, including 85 (55 in POS and 30 in NEG) up-regulated different metabolites and 24 (22 in POS and 2 in NEG) down-regulated different metabolites (Fig. 2C and D). 96 (66 in POS and 30 in NEG) different metabolites were detected in SYFS vs KBFS, including 81 (53 in POS and 28 in NEG) up-regulated different metabolites and 15 (13 in POS and 2 in NEG) down-regulated different metabolites (Fig. 2E and F). A total of 130 (93 in POS and 37 in NEG) different metabolites were detected in SYDB vs SYFS, including 77 (47 in POS and 30 in NEG) up-regulated different metabolites and 53 (46 in POS and 7 in NEG) down-regulated different metabolites (Fig. 2G and H).

Comparing SYDB to KBDB and SYFS to KBFS, we identified 39 (29 in POS and 10 in NEG) common differential metabolites (Fig. 3). In these common metabolites, 10.26 % were benzenoids, 17.95 % were organheterocyclic compounds, 20.51 % were organic oxygen compounds, 23.08 % were organic acids and derivatives, 12.82 % were lipids and lipid-like molecules, 2.56 % were phenylpropanoids and polyketides, and 12.82 % were other classes (Table 2). After conducting additional analysis, the top 10 metabolites with the same content of common differential metabolites between SYDB vs KBDB and SYFS vs KBFS were 3-α-galactobiose, maltose, maltotriose, melezitose, isomaltose, bispyribac, trehalose, palatinose, d-turanose, and thiodiglycol sulfoxide, eight of which were carbohydrates.

3.3. KEGG pathway

To further identify the metabolic pathways affected by low temperature stress, KEGG enrichment pathway analysis was performed

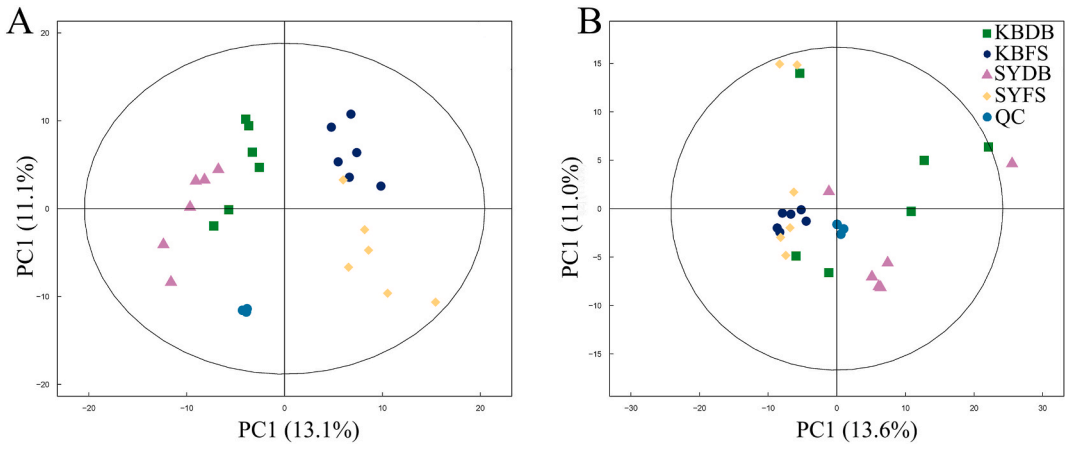

Fig. 1. (A) PCA analysis of overall samples in POS and (B) PCA analysis of overall samples in NEG.

Table 1
Evaluation parameters of the OPLS-DA model.

Groups	POS			NEG		
	R^2X	R^2Y	Q^2	R^2X	R^2Y	Q^2
SYDB vs SYFS	0.409	0.991	0.863	0.404	0.978	0.803
SYDB vs KBDB	0.373	0.995	0.788	0.244	0.992	0.485
SYFS vs KBFS	0.495	0.998	0.776	0.419	0.992	0.605
KBDB vs KBFS	0.376	0.985	0.819	0.526	0.983	0.641

R^2X denotes the explanatory rate of the model for the X variable; R^2Y denotes the explanatory rate of the model for the Y variable; and Q^2 denotes the predictive power of the model.

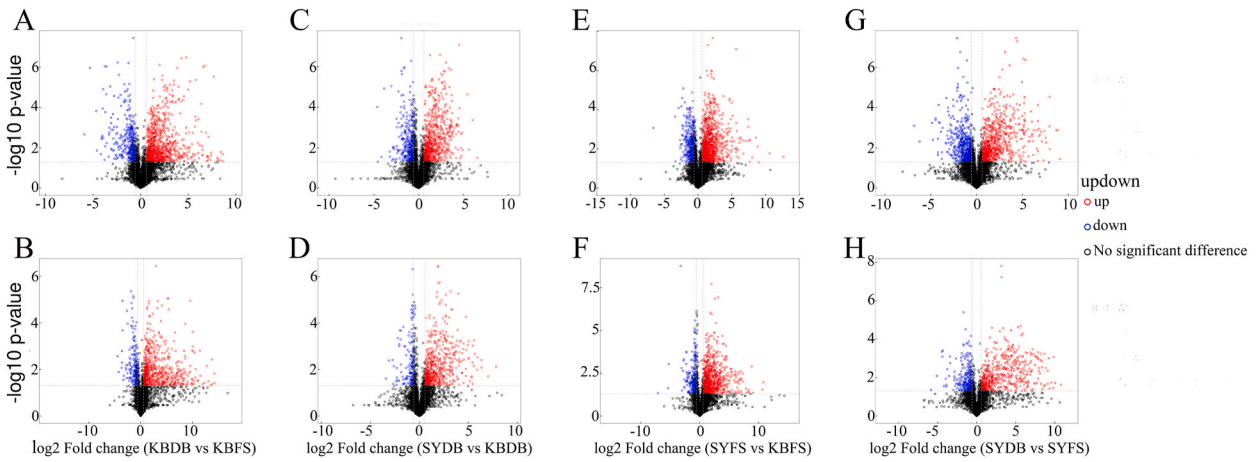

Fig. 2. (A) Volcano diagram of KBDB vs KBFS in POS; (B) Volcano diagram of KBDB vs KBFS in NEG; (C) Volcano diagram of SYDB vs KBDB in POS; (D) Volcano diagram of SYDB vs KBDB in NEG; (E) Volcano diagram of SYFS vs KBFS in POS; (F) Volcano diagram of SYFS vs KBFS in NEG; (G) Volcano diagram of SYDB vs SYFS in POS; (H) Volcano diagram of SYDB vs SYFS in NEG. The horizontal axis in the figure represents the logarithmic value of $\log_2$ for the fold change, while the vertical axis represents the logarithmic value of - $\log_{10}$ for the significance p value. Upregulated significant differential metabolites are represented in red, downregulated significant differential metabolites are represented in blue, and non-significant differential metabolites are represented in black. Volcano diagrams showed differential metabolites as FC > 1.5 or FC < 0.67, $P < 0.05$.

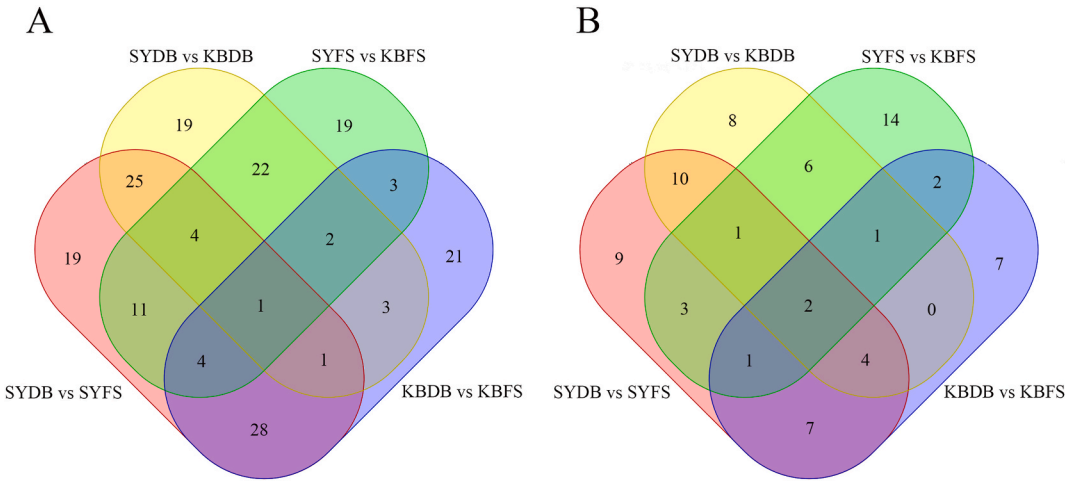

Fig. 3. (A) Venn diagram of overall samples in POS and (B) Venn diagram of overall samples in NEG.

on the screened differential metabolites. For SYDB vs. KBDB (Fig. 4A), a total of 14 metabolic pathways were enriched, primarily consisting of ABC transporters, starch and sucrose metabolism, and carbohydrate digestion and absorption. For SYFS vs. KBFS (Fig. 4B), a total of 31 metabolic pathways were enriched, primarily consisting of ABC transporters, purine metabolism, and phosphotransferase system (PTS). For SYDB vs. SYFS (Fig. 4C), 7 metabolic pathways were enriched, mostly consisting of ABC transporters,

Table 2
Differential metabolites shared by SYDB vs KBDB and SYFS vs KBFS.

SuperClass	Name	SYDB vs KBDB		SYFS vs KBFS	
		VIP	FC	VIP	FC
Benzenoids	1-(benzo[d] [1,3]dioxol-4-yl)-2-(methylamino)pentan-1-one	8.36	0.53	11.71	2.34
	1h-indole-5-sulfonamide,n-(3-chlorophenyl)-3-[[3,5-dimethyl-4-[(4-methyl-1-piperazinyl)carbonyl]-1h-pyrrol-2-yl]methylene]-2,3-dihydro-n-methyl-2-oxo-, (3z)-	1.47	3.46	1.96	22.45
	Procaine	1.47	4.64	1.33	7.08
	Pyridaben	1.39	4.04	1.33	5.22
Organheterocyclic compounds	1-deoxynojirimycin	1.15	3.67	1.11	3.53
	2-dimethylamino-6-hydroxypurine	2.11	2.70	2.13	3.80
	5-hydroxyindoleacetate	2.11	6.12	1.84	5.06
	Guanine	9.37	2.85	9.42	3.94
	Hypoxanthine	20.12	3.43	20.81	5.37
	Niacinamide	1.85	0.21	1.81	0.20
	Xanthine	1.95	9.82	2.14	21.27
Organic oxygen compounds	3-alpha-Galactobiose	1.37	94.38	2.72	6395.95
	Bispyribac	1.14	12.98	1.39	171.62
	Glutaraldehyde	1.30	4.97	2.08	11.82
	Maltotriose	8.67	12.74	10.67	1558.32
	Melezitose	2.33	20.35	2.69	513.00
	N-acetyl-d-glucosamine	1.17	0.28	2.91	0.20
	Trehalose	3.25	26.43	4.13	147.81
	4-alpha-mannobiose	2.53	0.35	1.09	98.73
Organic acids and derivatives	5-aminovaleric acid	1.91	1.77	3.05	3.30
	Cyclo-prolylglycine	1.56	1.57	1.86	2.21
	Dflnha	1.83	3.43	2.23	3.43
	Ethylenediaminetetraacetic acid	5.55	0.83	6.10	0.85
	Met-Met-Arg	1.05	0.63	1.33	1.91
	3-amino-1-propanesulfonic acid	5.49	3.43	1.12	1.88
	Dl-lactate	4.31	5.39	3.99	12.78
	Malate	1.36	6.20	1.48	11.18
	Succinate	1.54	2.67	1.77	6.46
Lipids and lipid-like molecules	Isomaltose	11.80	18.67	14.91	381.47
	Isovaleryl-l-carnitine	2.52	9.44	1.36	4.45
	D-turanose	1.33	23.16	2.37	123.00
	Maltose	2.91	44.76	5.00	1585.84
	Palatinose	1.09	32.61	1.85	136.76
Phenylpropanoids and polyketides	Tectoridin	4.63	9.09	1.65	0.01
Others	.beta.-Cyano-L-alanine	1.25	1.63	1.31	1.78
	5h-thieno [2,3-c]pyran-3-carboxylic acid, 2-[[(benzoylamino)thioxomethyl]amino]-4,7-dihydro-5,5-dimethyl-	1.36	12.59	1.46	25.19
	Thiodiglycol sulfoxide	4.89	43.95	6.19	108.30
	Tyr-Leu	13.14	9.85	10.30	5.09
	Zoniporide	2.38	8.95	1.70	3.97

protein digestion and absorption, and lysine degradation; KBDB vs. KBFS was not enriched in metabolic pathways. SYDB vs KBDB and SYFS vs KBFS had the same eight metabolic pathways, ABC transporters, carbohydrate digestion and absorption, starch and sucrose metabolism, lysine degradation, citrate cycle (TCA cycle), phosphotransferase system (PTS), glucagon signaling pathway and pyruvate metabolism, respectively.

3.4. Analysis of overall changes in KEGG pathway

The Differential Abundance Scores can capture the tendency for metabolites in a pathway to be increased (red)/decreased (blue) relative to controls [29]. SYDB vs KBDB enriched 14 metabolic pathways all tended to be up-regulated (Fig. 5A), 31 metabolic pathways enriched by SYFS vs KBFS all tended to be up-regulated (Fig. 5B), all 7 metabolic pathways enriched by SYDB vs SYFS tended to be down-regulated (Fig. 5C), and all 8 metabolic pathways shared between SYDB vs KBDB and SYFS vs KBFS also tended to be up-regulated.

4. Discussion

Extreme cold temperatures lead to the formation, growth, and recrystallization of intracellular ice crystals, which can be fatal to the organism [30]. A variety of differentially expressed metabolites of carbohydrates were found in both strains after experiencing low temperature incubation. The high concentration of glucose can act as an antifreeze protector and play an important role in preventing cell collapse, reducing cellular water loss, and decreasing the formation of ice crystals. This is one of the important antifreeze protection mechanisms in a variety of organisms [31–33]. The accumulation of trehalose, an important disaccharide involved in

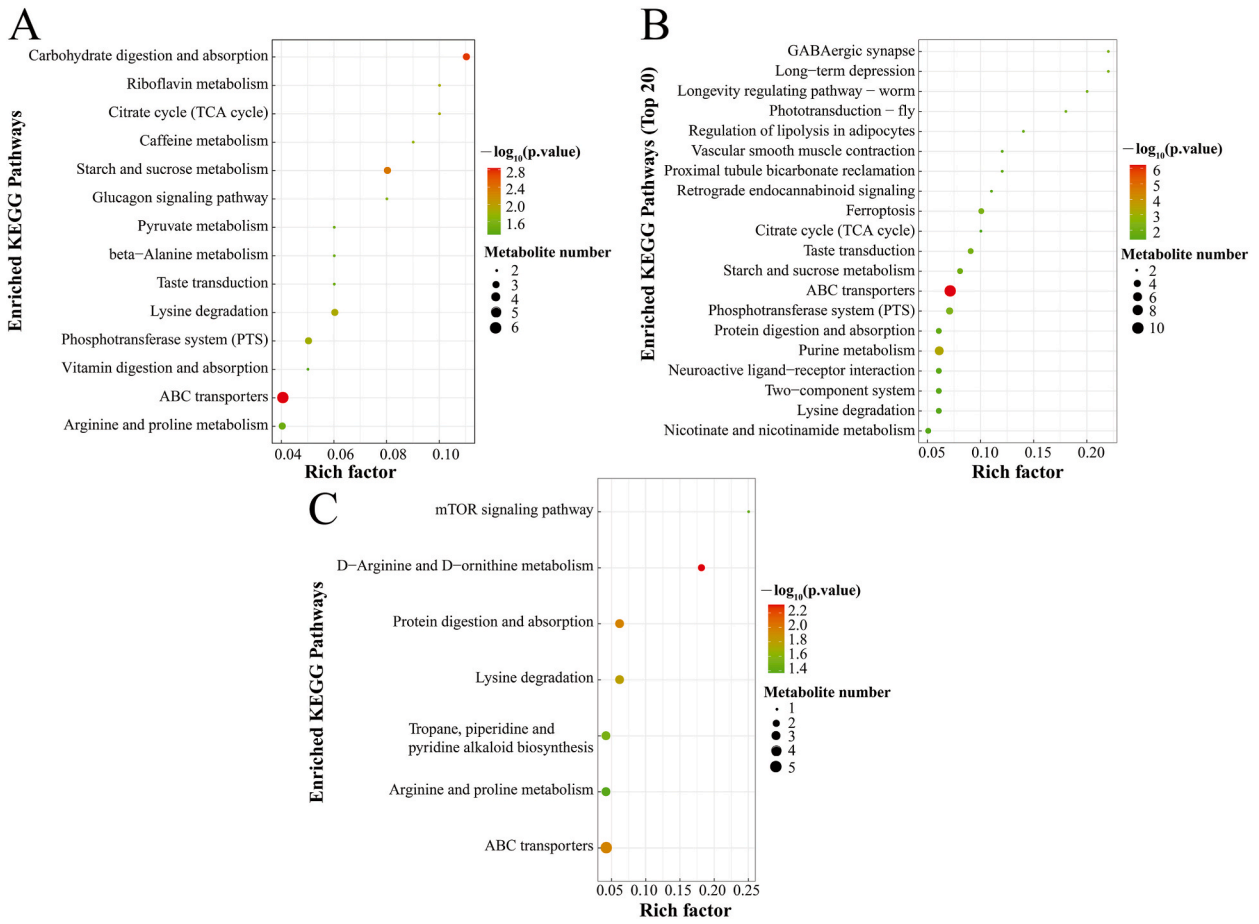

Fig. 4. Bubble diagram of metabolic pathways associated with differential metabolites (A) SYDB vs KBDB; (B) SYFS vs KBFS; (C) SYDB vs SYFS. Each bubble in the bubble map represents a metabolic pathway (the top 20 most significant ones were selected), and the size of the bubble is proportional to the impact value of the pathway in the topological analysis; the colour of the bubble indicates the degree of significance, the more colourful the bubble is, the smaller the *P*-value is, and the more significant the degree of enrichment is; the rich factor represents the number of differential metabolites of the pathway as a percentage of the number of metabolites annotated in the pathway.

adaptation to environmental stresses such as freezing, and used as a stabilizer of cellular structure under stressful conditions, is an important factor in coping with low-temperature stress [34,35], and has been applied to the cryopreservation of sturgeon semen [36]. Trehalose increases the flexibility of cell membranes and protects them and proteins from the effects of frostbite [37]. After a 24-h period of low-temperature stress, the trehalose level of Chinese mitten crab (*Eriocheir sinensis*) significantly increased, but glucose exhibited a trend of quick increase followed by a lengthy drop to withstand low-temperature stress [38]. With decreasing temperature, the trehalose content of *Gammarus fossarum* was significantly higher than the control level only at −2 °C ($P < 0.05$), and of all the carbohydrates detected, trehalose was the only one that accumulated [39]. It has been shown that the high concentration of carbohydrates in the process of low-temperature adaptation is a common characteristic of both cold- and freeze-resistant poikilotherms [40].

The carbohydrates may be the primary energy source in Pacific abalone during their response to low-temperature stress. Based on the KEGG-enriched pathway of differential metabolites, we have proposed a potential mechanism for the adaptation of Pacific abalone to low-temperature stress (Fig. 6). Polysaccharides ingested by abalone are digested by polysaccharide-degrading enzymes and further broken down into glucose [41,42]. The starch and sucrose metabolic pathways play a crucial role in the stress response by producing a variety of carbohydrates as metabolites to promote growth and the synthesis of essential compounds [43], such as trehalose biosynthesis. Starch and sucrose can be broken down into glucose, which provides the body with energy quickly [44]. It was discovered that fish have disruptions in their energy metabolism when exposed to low temperature conditions, so their starch and sucrose metabolism pathways become active in an attempt to make up for this energy deficit [45,46]. After undergoing final hydrolysis, glucose is converted to pyruvate and then oxidized to acetyl CoA, which starts the TCA cycle. With the help of the body's enzymes, L-lysine first produces 5-Aminopentanoate, which then produces succinate, which is used in the TCA cycle. As the body's counter-regulatory hormone to insulin, glucagon is essential for preserving glucose homeostasis [47]. Glucagon is released when there is a low level of circulating glucose, which elevates plasma glucose levels [48]. ABC transporters are a class of membrane-integrated proteins that are widely present in organisms, catalyze the hydrolysis of ATP, and use the energy generated by the hydrolysis to

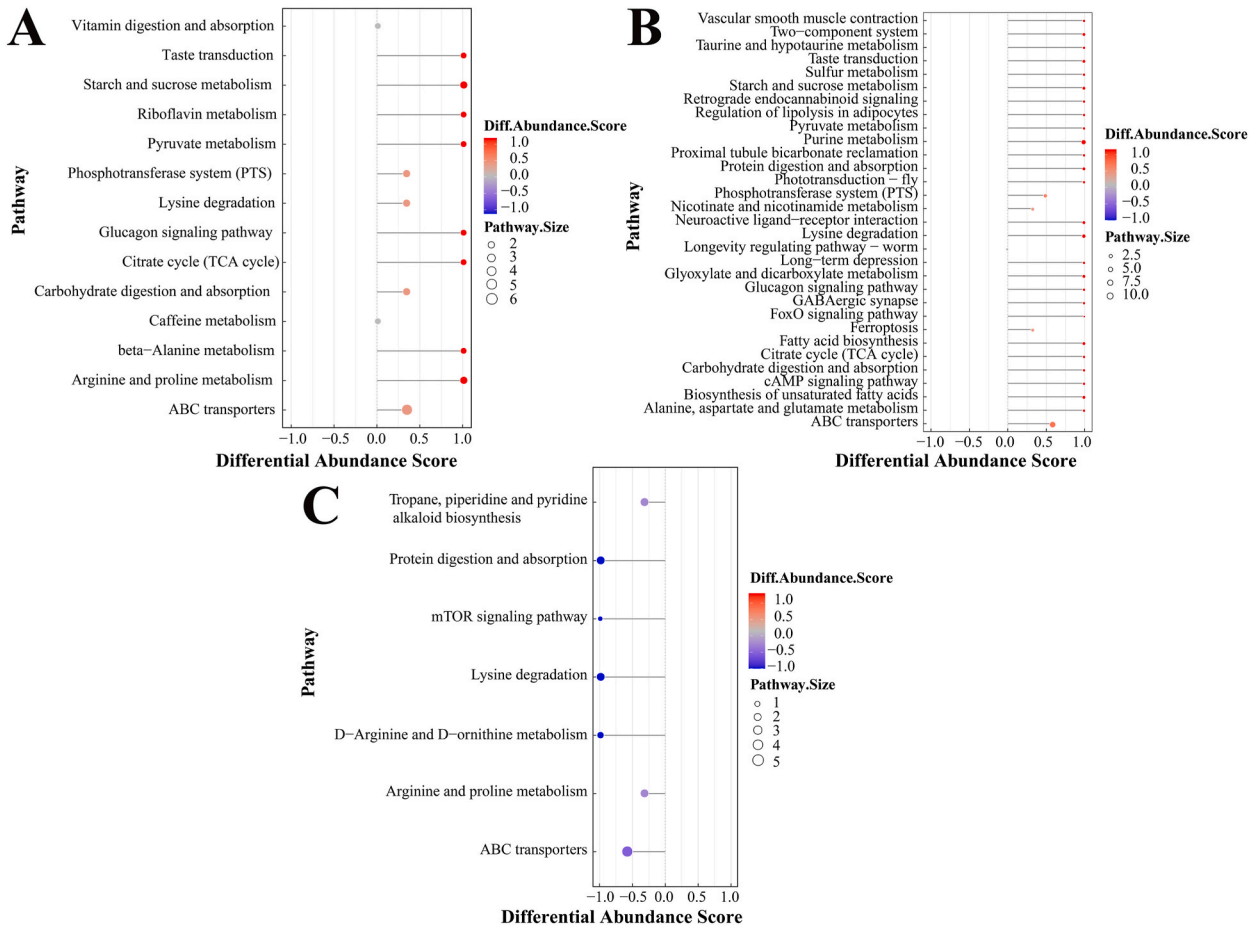

Fig. 5. Differential metabolite-related metabolic pathway differential abundance score map. (A) SYDB vs KBDB; (B) SYFS vs KBFS; (C) SYDB vs SYFS.

facilitate the transmembrane transfer of substrates, and are a part of membrane transport [49]. These proteins' primary roles include controlling cellular osmolality, transporting lipids and cholesterol across membranes, and transporting biomolecules [50]. It has been shown that ABC transporters may play an important role in the transport of small molecules during the cryogenic activity of large yellow croaker (*Larimichthys crocea*) and are involved in energy metabolism [51]. ABC transporters can use the energy obtained from ATP hydrolysis for transmembrane transport of biomolecules, and is involved in physiological functions such as cellular osmotic pressure regulation, lipid and cholesterol transport, cellular differentiation, and antigen presentation [52]. The Phosphotransferase system (PTS) is a system that transports and simultaneously phosphorylates carbohydrates [53], and phosphorylates various carbohydrates and their derivatives mainly through a phosphate cascade reaction and then transports them to the intracellular compartment for the next step of catabolism [54,55]. The TCA cycle is the primary metabolic pathway by which organisms oxidize carbohydrates and other substances for energy [56–58]. It is also the last metabolic pathway for the three major nutrients in the organism. Furthermore, the metabolic intermediates of the TCA cycle have critical roles in biological development and the maintenance of cellular homeostasis [59]. Citric acid is the first intermediate product in the TCA cycle and an increase in citric acid is an important signal to inhibit catabolic reactions and favor anabolic reactions [60]. Succinic acid and malic acid are also key intermediates in the TCA cycle, while succinic acid promotes the hydrolysis of brown fat and releases energy, which in turn provides heat to the organism [61]. Massive and selective accumulation of succinate, an intermediate of the tricarboxylic acid cycle, characterizes the metabolism of adipose tissue for thermogenesis after activation by exposure to cold, and it is involved in the regulation of glycolipid metabolism as an energy substance. Succinate from the extracellular environment is rapidly metabolized by brown adipocytes, and its oxidation by succinate dehydrogenase is required for the activation of thermogenesis [62,63]. Most significantly, the TCA cycle produces energy with high efficiency, which helps the organism withstand adverse environments like cold [64].

Acute changes in temperature conditions alter the energy metabolic pathways of organisms [65]. For example, *Leiocassis longirostris* adapted to low-temperature stress by activating related lipid synthesis and metabolism [66]. *Raphidiopsis raciborskii* had a lower energy requirement in low-temperature environments but increased the production of carbohydrates and glycans to maintain cell membrane stability or withstand oxidative stress [67]. Juvenile sea bass (*Dicentrarchus labrax*) adapted to low-temperature stress through lipid metabolism, glucose metabolism, and the tricarboxylic acid cycle [68]. Temperature affects metabolomic pathways related to the

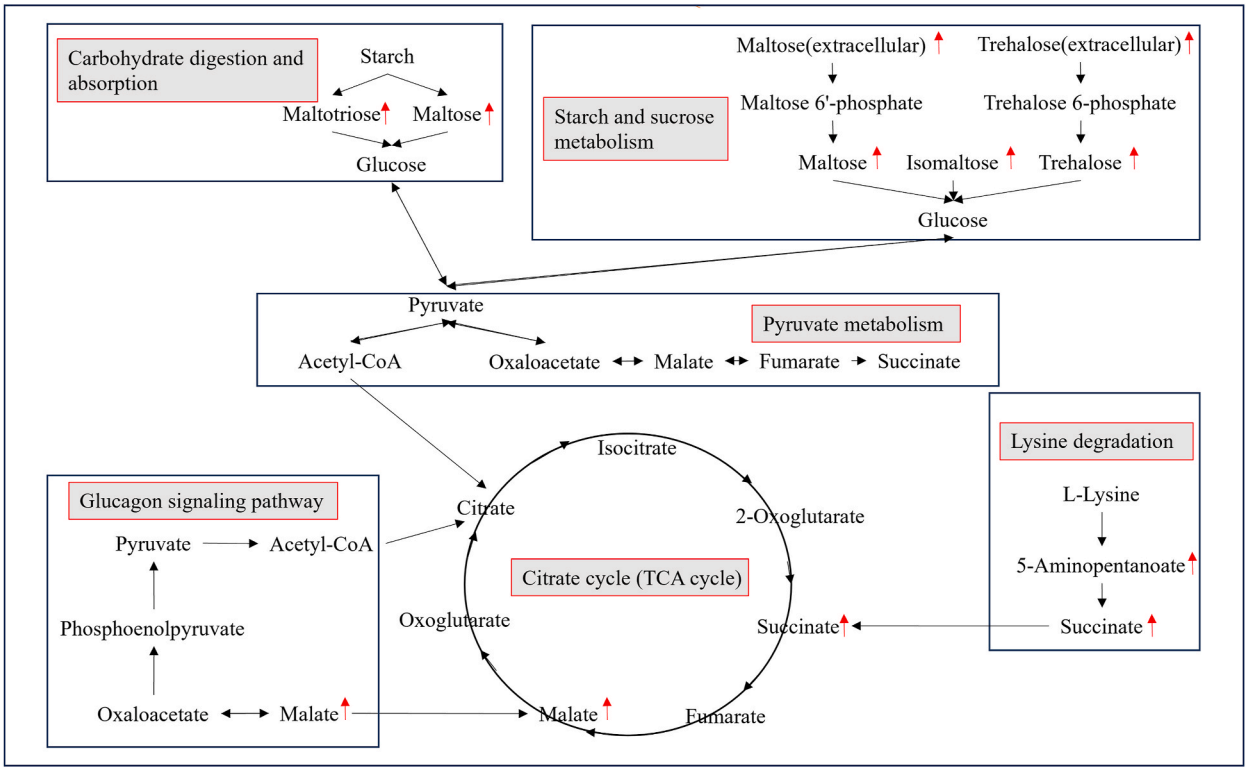

Fig. 6. Predictive model of the metabolic response of Pacific abalone (*Haliotis discus hannai*) to low-temperature stress.

tricarboxylic acid cycle and amino acid metabolism in northern shrimp (*Pandalus borealis*) [69], and shellfish may be resistant to temperature changes through energy metabolism [70]. In line with the findings of the study on Ulva prolifera's low temperature tolerance [71], we discovered that the majority of carbohydrate-related metabolites were consistently up-regulated in our investigation.

Furthermore, we also noticed that SYDB vs KBDB had far fewer metabolic enrichment pathways than SYFS vs KBFS, and all seven metabolic enrichment pathways tended to be downregulated in SYDB vs SYFS. It has been shown that two groups of Pacific abalone (*Haliotis discus hannai*) experiencing different acclimatization temperatures (10 °C and 30 °C for 62 days) exhibited significantly different survival rates under an acute heat treatment at 31 °C, and that high-temperature acclimatization may have had a specific effect on the metabolic processes of abalone, allowing them to make beneficial physiological responses when exposed to heat stress, which in turn makes them more likely to survive in harsh environments [14].Similarly our previous findings showed that the bottom-sowing abalone that have experienced low-temperature stress accumulate more total carbohydrates [19]. We suggest that this accumulation of carbohydrates appears to make the abalone more resilient to low-temperature stress, allowing them to survive in a more energy-efficient metabolic manner. Although the mechanism needs more clarification, this study may be helpful in providing insights into the energy metabolism of the Pacific abalone under low-temperature stress. Meanwhile, we suggest exploring other temperature ranges, assessing the long-term effects of cold stress, or investigating genetic factors influencing metabolic responses in order to gain a comprehensive understanding of the coping mechanisms of the abalone to low-temperature stress. This research can provide a scientific basis for optimizing the aquaculture strategy.

5. Conclusions

In this study, we used ultrahigh-performance liquid chromatography coupled with quadrupole time-of-flight mass spectrometry (UHPLC-Q-TOF-MS) to investigate the metabolic reactions of the Pacific abalone (*Haliotis discus hannai*) to low-temperature stress. It was found that the abalone organism responded to the low temperature by increasing its production of carbohydrates. While glucose ultimately broke down and participated in the TCA cycle, thereby increasing the available energy, small molecular carbohydrates can also be employed as antifreeze protectants to shield proteins and cell membranes from harm. Additionally, we observed a slightly different metabolic response to low-temperature stress between longline cultured abalone and bottom-sowing cultured abalone. These results could offer novel perspectives on the abalone's acclimation to cold temperatures and can help optimize culture strategies for high-quality abalone aquaculture development.

CRediT authorship contribution statement

Ang Li: Writing – original draft, Formal analysis, Data curation. **Jiaqi Li:** Writing – review & editing, Funding acquisition, Conceptualization. **Yingpu Wang:** Investigation, Formal analysis. **Zirong Liu:** Investigation, Formal analysis. **Lulei Liu:** Investigation, Formal analysis. **Longzhen Liu:** Investigation, Formal analysis. **Suyan Xue:** Writing – review & editing. **Ling Zhu:** Writing – review & editing. **Yuze Mao:** Writing – review & editing, Funding acquisition.

Data availability

Data will be made available on request.

Declaration of competing interest

The authors declare that they have no known competing financial interests or personal relationships that could have appeared to influence the work reported in this paper.

Acknowledgements

This work was supported by the National Key R&D Program of China (2023YFD2400800, SQ2024YFD2400015), Central Public-interest Scientific Institution Basal Research Fund, YSFRI, CAFS (NO.2023TD54, NO.20603022023007), Shandong Province Science and Technology based Small and Medium sized Enterprises Innovation Capability Enhancement Project (2023TSGC0768). We express our gratitude to Xunshan Group for supplying the samples of abalone. Metabolomics analysis of this work was completed at Applied Protein Technology, Shanghai, China.

Appendix A. Supplementary data

Supplementary data to this article can be found online at https://doi.org/10.1016/j.heliyon.2024.e40921.

References

[1] N.L. Ward, G.J. Masters, Linking climate change and species invasion: an illustration using insect herbivores, Global Change Biol. 13 (8) (2007) 1605–1615, https://doi.org/10.1111/j.1365-2486.2007.01399.x.
[2] L.B. Firth, A.M. Knights, S.S. Bell, Air temperature and winter mortality: implications for the persistence of the invasive mussel, Perna viridis in the intertidal zone of the south-eastern United States, J. Exp. Mar. Biol. Ecol. 400 (1) (2011) 250–256, https://doi.org/10.1016/j.jembe.2011.02.007.
[3] A. Simon, S.M. Plecha, A.C. Russo, A. Teles-Machado, M.G. Donat, P. Auger, R.M. Trigo, Hot and cold marine extreme events in the Mediterranean over the period 1982-2021, Front. Mar. Sci. 9 (2022) 892201, https://doi.org/10.3389/fmars.2022.892201.
[4] O. Hoegh-Guldberg, J.F. Bruno, The impact of climate change on the world's marine ecosystems, Science 328 (5985) (2010) 1523–1528, https://doi.org/10.1126/science.1189930.
[5] J.P. Gattuso, A.K. Magnan, L. Bopp, W.W.L. Cheung, C.M. Duarte, J. Hinkel, E. Mcleod, F. Micheli, A. Oschlies, P. Williamson, R. Billé, V.I. Chalastani, R. D. Gates, J.O. Irisson, J.J. Middelburg, H.-O. Pörtner, G.H. Rau, Ocean solutions to address climate change and its effects on marine ecosystems, Front. Mar. Sci. Front. Mar. Sci. 5 (2018) 337, https://doi.org/10.3389/fmars.2018.00337.
[6] T.V. Nguyen, A.C. Alfaro, Metabolomics investigation of summer mortality in New Zealand Greenshell™ mussels (*Perna canaliculus*), Fish Shellfish Immunol. 106 (2020) 783–791, https://doi.org/10.1016/j.fsi.2020.08.022.
[7] R.W. Schlegel, S. Darmaraki, J.A. Benthuysen, K. Filbee-Dexter, E.C.J. Oliver, Marine cold-spells, Prog. Oceanogr. 198 (2021) 102684, https://doi.org/10.1016/j.pocean.2021.102684.
[8] D.W. Kemp, C.A. Oakley, D.J. Thornhill, L.A. Newcomb, G.W. Schmidt, W.K. Fitt, Catastrophic mortality on inshore coral reefs of the Florida Keys due to severe low-temperature stress, Global Change Biol. 17 (11) (2011) 3468–3477, https://doi.org/10.1111/j.1365-2486.2011.02487.x.
[9] R.O. Santos, J.S. Rehage, R. Boucek, J. Osborne, Shift in recreational fishing catches as a function of an extreme cold event, Ecosphere 7 (6) (2016) e01335, https://doi.org/10.1002/ecs2.1335.
[10] H. Luo, J. Xiao, Y. Jiang, Y. Ke, C. Ke, M. Cai, Mapping and marker identification for sex-determining in the Pacific abalone, Haliotis discus hannai Ino, Aquaculture 530 (2021) 735810, https://doi.org/10.1016/j.aquaculture.2020.735810.
[11] W. Yu, L. Zeng, W. Zou, Y. Shu, J.C. Gwo, W. You, X. Luo, C. Ke, Seasonal variation in the nutritional components and textural properties of Pacific abalone and its hybrids, Aquaculture 563 (2023) 738930, https://doi.org/10.1016/j.aquaculture.2022.738930.
[12] H.A.R. Suleria, P.P. Masci, G.C. Gobe, S.A. Osborne, Therapeutic potential of abalone and status of bioactive molecules: a comprehensive review, Crit. Rev. Food Sci. Nutr. 57 (8) (2017) 1742–1748, https://doi.org/10.1080/10408398.2015.1031726.
[13] K. Lei, C. Liu, J. Sahandi, Z. Cui, W. Rao, P. Chen, B.B. Tabuariki, K. Mai, W. Zhang, Effects of dietary eicosapentaenoic acid on the growth performance, fatty acid profile, immunity and heat tolerance of juvenile abalone *Haliotis discus hannai* Ino, Aquaculture 578 (2024) 740015, https://doi.org/10.1016/j.aquaculture.2023.740015.
[14] F. Xu, T. Gao, X. Liu, Metabolomics adaptation of juvenile pacific abalone Haliotis discus hannai to heat stress, Sci. Rep. 10 (1) (2020) 6353, https://doi.org/10.1038/s41598-020-63122-4.
[15] D.S. Wethey, S.A. Woodin, T.J. Hilbish, S.J. Jones, F.P. Lima, P.M. Brannock, Response of intertidal populations to climate: effects of extreme events versus long term change, J. Exp. Mar. Biol. Ecol. 400 (1) (2011) 132–144, https://doi.org/10.1016/j.jembe.2011.02.008.
[16] V.V. Tolstikov, O. Fiehn, Analysis of highly polar compounds of plant origin: combination of hydrophilic interaction chromatography and electrospray ion trap mass spectrometry, Anal. Biochem. 301 (2) (2002) 298–307, https://doi.org/10.1006/abio.2001.5513.
[17] J.K. Nicholson, I.D. Wilson, Understanding 'global' systems biology: metabonomics and the continuum of metabolism, Nat. Rev. Drug Discov. 2 (8) (2003) 668–676, https://doi.org/10.1038/nrd1157.

[18] T.V. Nguyen, A. Alfaro, E. Frost, D. Chen, D.J. Beale, C. Mundy, Investigating the biochemical effects of heat stress and sample quenching approach on the metabolic profiling of abalone (*Haliotis iris*), Metabolomics 18 (1) (2021) 7, https://doi.org/10.1007/s11306-021-01862-8.

[19] Y.P. Wang, J.Q. Li, S.Y. Xue, Z.F. Ma, L.R. Chang, L.F. Lu, Y.T. Zhang, Y.Z. Mao, Effects of two farming models on the biochemical composition and response to low temperature stress of *Haliotis discus hannai*, Prog. Fish. Sci. 44 (5) (2023) 202–210, https://doi.org/10.19663/j.issn2095-9869.20220310003.

[20] D. Broadhurst, R. Goodacre, S.N. Reinke, J. Kuligowski, I.D. Wilson, M.R. Lewis, W.B. Dunn, Guidelines and considerations for the use of system suitability and quality control samples in mass spectrometry assays applied in untargeted clinical metabolomic studies, Metabolomics 14 (6) (2018) 72, https://doi.org/10.1007/s11306-018-1367-3.

[21] Y.W. Cao, R.J. Qu, Y.J. Miao, X.Q. Tang, Y. Zhou, L. Wang, L. Geng, Untargeted liquid chromatography coupled with mass spectrometry reveals metabolic changes in nitrogen-deficient Isatis indigotica Fortune, Phytochemistry 166 (2019) 112058, https://doi.org/10.1016/j.phytochem.2019.112058.

[22] F.P.S. Reginaldo, P.C.P. Bueno, E.M.G. Lourenço, I.C. de Matos Costa, L.G.L. Moreira, A. de Araújo Roque, E.G. Barbosa, A.G. Fett-Neto, A.J. Cavalheiro, R. B. Giordani, Methyl jasmonate induces selaginellin accumulation in Selaginella convoluta, Metabolomics 19 (1) (2022) 2, https://doi.org/10.1007/s11306-022-01966-9.

[23] E. Gaude, F. Chignola, D. Spiliotopoulos, A. Spitaleri, M. Ghitti, J.M. Garcia-Manteiga, S. Mari, G. Musco, Muma, an R package for metabolomics univariate and multivariate statistical analysis, Curr. Metabolomics 1 (2) (2013) 180–189, https://doi.org/10.2174/2213235X11301020005.

[24] F. Xue, X. Pan, L. Jiang, Y. Guo, B. Xiong, GC–MS analysis of the ruminal metabolome response to thiamine supplementation during high grain feeding in dairy cows, Metabolomics 14 (5) (2018) 67, https://doi.org/10.1007/s11306-018-1362-8.

[25] Z. Gu, L. Li, S. Tang, C. Liu, X. Fu, Z. Shi, H. Mao, Metabolomics reveals that crossbred dairy buffaloes are more thermotolerant than holstein cows under chronic heat stress, J. Agric. Food Chem. 66 (49) (2018) 12889–12897, https://doi.org/10.1021/acs.jafc.8b02862.

[26] D. Luo, T. Deng, W. Yuan, H. Deng, M. Jin, Plasma metabolomic study in Chinese patients with wet age-related macular degeneration, BMC Ophthalmol. 17 (1) (2017) 165, https://doi.org/10.1186/s12886-017-0555-7.

[27] I. Blaženović, T. Kind, J. Ji, O. Fiehn, Software tools and approaches for compound identification of LC-MS/MS data in metabolomics, Metabolites 8 (2) (2018), https://doi.org/10.3390/metabo8020031.

[28] Z.Q. Pang, J. Chong, G.Y. Zhou, D.A.D.L. Morais, L. Chang, M. Barrette, C. Gauthier, P.É. Jacques, S.Z. Li, J.G. Xia, MetaboAnalyst 5.0: narrowing the gap between raw spectra and functional insights, Nucleic Acids Res. 49 (W1) (2021) W388–W396, https://doi.org/10.1093/nar/gkab382.

[29] A.A. Hakimi, E. Reznik, C.-H. Lee, C.J. Creighton, A.R. Brannon, A. Luna, B.A. Aksoy, E.M. Liu, R. Shen, W. Lee, Y. Chen, S.M. Stirdivant, P. Russo, Y.-B. Chen, S. K. Tickoo, V.E. Reuter, E.H. Cheng, C. Sander, J.J. Hsieh, An integrated metabolic atlas of clear cell renal cell carcinoma, Cancer Cell 29 (1) (2016) 104–116, https://doi.org/10.1016/j.ccell.2015.12.004.

[30] C. Tie, Z. Gang, Ice inhibition for cryopreservation: materials, strategies, and challenges, Adv. Sci. 8 (6) (2021) 2002425, https://doi.org/10.1002/advs.202002425.

[31] J.P. Costanzo, R.E.J.R. Lee, P.H. Lortz, Glucose concentration regulates freeze tolerance in the wood frog Rana sylvatica, J. Exp. Biol. 181 (1) (1993) 245–255, https://doi.org/10.1242/jeb.181.1.245.

[32] Y. Park, Y. Kim, A specific glycerol kinase induces rapid cold hardening of the diamondback moth, Plutella xylostella, J. Insect Physiol. 67 (2014) 56–63, https://doi.org/10.1016/j.jinsphys.2014.06.010.

[33] S.S. Dong, H.T. Nie, X.W. Yan, Research progresses on mechanisms of cold stress responses in shellfish: a review, J. Dalian Ocean Univ. 34 (3) (2019) 457–462, https://doi.org/10.16535/j.cnki.dlhyxb.2019.03.023.

[34] J.H. Crowe, L.M. Crowe, D. Chapman, Preservation of membranes in anhydrobiotic organisms: the role of trehalose, Science 223 (4637) (1984) 701–703, https://doi.org/10.1126/science.223.4637.701.

[35] B. Tang, X. Chen, Y. Liu, H. Tian, J. Liu, J. Hu, W. Xu, W. Zhang, Characterization and expression patterns of a membrane-bound trehalase from Spodoptera exigua, BMC Mol. Biol. 9 (1) (2008) 51, https://doi.org/10.1186/1471-2199-9-51.

[36] K. Golshahi, M.S. Aramli, R.M. Nazari, E. Habibi, Disaccharide supplementation of extenders is an effective means of improving the cryopreservation of semen in sturgeon, Aquaculture 486 (2018) 261–265, https://doi.org/10.1016/j.aquaculture.2017.12.045.

[37] V. Koštál, J. Korbelová, J. Rozsypal, H. Zahradníčková, J. Cimlová, A. Tomčala, P. Šimek, Long-term cold acclimation extends survival time at 0°C and modifies the metabolomic profiles of the larvae of the fruit fly Drosophila melanogaster, PLoS One 6 (9) (2018) e25025.

[38] J. Bao, X. Wang, C. Feng, X. Li, H. Jiang, Trehalose metabolism in the Chinese mitten crab Eriocheir sinensis: molecular cloning of trehalase and its expression during temperature stress, Aquacult. Rep. 20 (2021) 100770, https://doi.org/10.1016/j.aqrep.2021.100770.

[39] J. Issartel, D. Renault, Y. Voituron, A. Bouchereau, P. Vernon, F.d.r. Hervant, Metabolic responses to cold in subterranean crustaceans, J. Exp. Biol. 208 (15) (2005) 2923–2929, https://doi.org/10.1242/jeb.01737.

[40] M.V. Karanova, E.N. Gakhova, Biochemical strategy of survival of the freshwater mollusc Lymnaea stagnalis at near-zero temperatures, J. Evol. Biochem. Physiol. 43 (3) (2007) 310–317, https://doi.org/10.1134/S0022093007030052.

[41] T. Ojima, M.M. Rahman, Y. Kumagai, R. Nishiyama, J. Narsico, A. Inoue, Polysaccharide-degrading enzymes from marine gastropods, Methods Enzymol. 605 (2018) 457–497, https://doi.org/10.1016/bs.mie.2018.01.032.

[42] L. Drozdowski, A. Thomson, Intestinal sugar transport, World J. Gastroenterol. 12 (2006) 1657–1670, https://doi.org/10.3748/wjg.v12.i11.1657.

[43] Y.-L. Ruan, Sucrose metabolism: gateway to diverse carbon use and sugar signaling, Annu. Rev. Plant Biol. 65 (1) (2014) 33–67, https://doi.org/10.1146/annurev-arplant-050213-040251.

[44] L. Zeng, W. Song, Z.L. Xie, Y.H. Wang, Y.F. Xiong, H. Zhang, Metabolomics-based analysis of adaptive mechanism of *Larimichthys crocea* to low temperature and starvation stresses, J. Fish. China 47 (7) (2023) 88–99.

[45] S. Jiao, M. Nie, H. Song, D. Xu, F. You, Physiological responses to cold and starvation stresses in the liver of yellow drum (Nibea albiflora) revealed by LC-MS metabolomics, Sci. Total Environ. 715 (2020) 136940, https://doi.org/10.1016/j.scitotenv.2020.136940.

[46] B. Wen, S.-R. Jin, Z.-Z. Chen, J.-Z. Gao, Physiological responses to cold stress in the gills of discus fish (Symphysodon aequifasciatus) revealed by conventional biochemical assays and GC-TOF-MS metabolomics, Sci. Total Environ. 640–641 (2018) 1372–1381, https://doi.org/10.1016/j.scitotenv.2018.05.401.

[47] G. Jiang, B.B. Zhang, Glucagon and regulation of glucose metabolism, Am. J. Physiol. Endocrinol. Metab. 284 (4) (2003) E671–E678, https://doi.org/10.1152/ajpendo.00492.2002.

[48] L. Freychet, N. Desplanque, P. Zirinis, S.W. Rizkalla, A. Basdevant, G. Tchobroutsky, G. Slama, EFFECT of intranasal glucagon on blood glucose levels in healthy subjects and hypoglycaemic patients with insulin-dependent diabetes, Lancet 331 (8599) (1988) 1364–1366, https://doi.org/10.1016/S0140-6736(88)92181-2.

[49] K.P. Locher, Structure and mechanism of ATP-binding cassette transporters, Philos. Trans. R. Soc. Lond. B Biol. Sci. 364 (1514) (2008) 239–245, https://doi.org/10.1098/rstb.2008.0125.

[50] H. Yao, X. Li, L.S. Tang, H. Wang, C. Wang, C.K. Mu, C. Shi, Metabolic mechanism of the mud crab (Scylla paramamosain) adapting to salinity sudden drop based on GC-MS technology, Aquacult. Rep. 18 (2020) 100533, https://doi.org/10.1016/j.aqrep.2020.100533.

[51] H. Lv, X. Qu, Z. Chu, W. Li, X. Yin, D. Feng, J. Park, J. Hur, Y. Gao, Integration of transcriptomics and metabolomics reveals the effects of sea currents on overwintering of large yellow croaker Larimichthys crocea in cage culture, Aquaculture 578 (2024) 740054, https://doi.org/10.1016/j.aquaculture.2023.740054.

[52] P.M. Jones, A.M. George, The ABC transporter structure and mechanism: perspectives on recent research, Cell. Mol. Life Sci. 61 (6) (2004) 682–699.

[53] W. Kundig, S. Ghosh, S. Roseman, Phosphate bound to histidine in a protein as an intermediate in a novel phospho-transferase system, Proc. Natl. Acad. Sci. U.S. A. 52 (4) (1964) 1067–1074, https://doi.org/10.1073/pnas.52.4.1067.

[54] J. Deutscher, C. Francke, W. Postma Pieter, How phosphotransferase system-related protein phosphorylation regulates carbohydrate metabolism in bacteria, Microbiol. Mol. Biol. Rev. 72 (3) (2008) 555, https://doi.org/10.1128/mmbr.00018-08, 555.

[55] Q.Y. Liu, L.W. Wu, J.J. Niu, X.L. Zhao, Research progress of the composition and function of bacterial phosphotransferase system, Microbiol. China 47 (7) (2020) 2266–2277, https://doi.org/10.13344/j.microbiol.china.200134.

[56] W. Kang, M. Suzuki, T. Saito, K. Miyado, Emerging role of TCA cycle-related enzymes in human diseases, Int. J. Mol. Sci. 22 (23) (2021) 13057, https://doi.org/10.3390/ijms222313057.
[57] I. Martínez-Reyes, Lauren P. Diebold, H. Kong, M. Schieber, H. Huang, Christopher T. Hensley, Manan M. Mehta, T. Wang, Janine H. Santos, R. Woychik, E. Dufour, Johannes N. Spelbrink, Samuel E. Weinberg, Y. Zhao, Ralph J. DeBerardinis, Navdeep S. Chandel, TCA cycle and mitochondrial membrane potential are necessary for diverse biological functions, Mol Cell 61 (2) (2016) 199–209, https://doi.org/10.1016/j.molcel.2015.12.002.
[58] Y. Zhang, K.F.M. Beard, C. Swart, S. Bergmann, I. Krahnert, Z. Nikoloski, A. Graf, R.G. Ratcliffe, L.J. Sweetlove, A.R. Fernie, T. Obata, Protein-protein interactions and metabolite channelling in the plant tricarboxylic acid cycle, Nat. Commun. 8 (1) (2017) 15212, https://doi.org/10.1038/ncomms15212.
[59] M. Akram, Citric acid cycle and role of its intermediates in metabolism, Cell Biochem. Biophys. 68 (3) (2014) 475–478, https://doi.org/10.1007/s12013-013-9750-1.
[60] C. Frezza, Mitochondrial metabolites: undercover signalling molecules, Interface Focus 7 (2) (2017) 20160100, https://doi.org/10.1098/rsfs.2016.0100.
[61] H. Sheng, R.J. D, An unexpected trigger for calorie burning in brown fat, Nature 560 (7716) (2018) 38–39, https://doi.org/10.1038/d41586-018-05619-7.
[62] E.L. Mills, K.A. Pierce, M.P. Jedrychowski, R. Garrity, S. Winther, S. Vidoni, T. Yoneshiro, J.B. Spinelli, G.Z. Lu, L. Kazak, A.S. Banks, M.C. Haigis, S. Kajimura, M.P. Murphy, S.P. Gygi, C.B. Clish, E.T. Chouchani, Accumulation of succinate controls activation of adipose tissue thermogenesis, Nature 560 (2018) 102–106.
[63] M.Y. Li, Z.G. Wang, S. Liu, H. Lin, H.F. Li, Succinate:a pleiotropic metabolite in energy homeostasis, Chin. Bull. Life Sci. 35 (9) (2023) 1128–1135.
[64] Deborah M. Muoio, Metabolic inflexibility: when mitochondrial indecision leads to metabolic gridlock, Cell 159 (6) (2014) 1253–1262, https://doi.org/10.1016/j.cell.2014.11.034.
[65] A. Aguilar, H. Mattos, B. Carnicero, N. Sanhueza, D. Muñoz, M. Teles, L. Tort, S. Boltaña, Metabolomic profiling reveals changes in amino acid and energy metabolism pathways in liver, intestine and brain of zebrafish exposed to different thermal conditions, Front. Mar. Sci. 9 (2022), https://doi.org/10.3389/fmars.2022.835379.
[66] M. Liu, Y.L. Zhou, X.F. Guo, W.Y. Wei, Z. Li, L. Zhou, Z.W. Wang, J.-F. Gui, Comparative transcriptomes and metabolomes reveal different tolerance mechanisms to cold stress in two different catfish species, Aquaculture 560 (2022) 738543, https://doi.org/10.1016/j.aquaculture.2022.738543.
[67] B. Zheng, S. He, L. Zhao, J. Li, Y. Du, Y. Li, J. Shi, Z. Wu, Does temperature favour the spread of Raphidiopsis raciborskii, an invasive bloom-forming cyanobacterium, by altering cellular trade-offs? Harmful Algae 124 (2023) 102406 https://doi.org/10.1016/j.hal.2023.102406.
[68] C. Zhou, Z.Q. Zhang, L. Zhang, Y. Liu, P.F. Liu, Effects of temperature on growth performance and metabolism of juvenile sea bass (*Dicentrarchus labrax*), Aquaculture 537 (2021) 736458, https://doi.org/10.1016/j.aquaculture.2021.736458.
[69] E. Guscelli, D. Chabot, F. Vermandele, D. Madeira, P. Calosi, All roads lead to Rome: inter-origin variation in metabolomics reprogramming of the northern shrimp exposed to global changes leads to a comparable physiological status, Front. Mar. Sci. 10 (2023), https://doi.org/10.3389/fmars.2023.1170451.
[70] K. Jahan, H. Nie, Z. Yin, Y. Zhang, N. Li, X. Yan, Comparative transcriptome analysis to reveal the genes and pathways associated with adaptation strategies in two different populations of Manila clam (Ruditapes philippinarum) under acute temperature challenge, Aquaculture 552 (2022) 737999, https://doi.org/10.1016/j.aquaculture.2022.737999.
[71] Y. He, Y. Wang, C. Hu, W. Hu, W. Zhu, N. Xu, Potential biomarkers of low-temperature tolerance in Ulva prolifera strains, J. Appl. Phycol. 34 (2) (2022) 1099–1108, https://doi.org/10.1007/s10811-021-02666-y.